

Cite this: *Nanoscale*, 2015, **7**, 16389

## Double loaded self-decomposable $\text{SiO}_2$ nanoparticles for sustained drug release†

Saisai Zhao,‡<sup>a</sup> Silu Zhang,‡<sup>a</sup> Jiang Ma,<sup>b</sup> Li Fan,<sup>a,c</sup> Chun Yin,<sup>b</sup> Ge Lin<sup>b</sup> and Quan Li\*<sup>a</sup>

Sustained drug release for a long duration is a desired feature of modern drugs. Using double-loaded self-decomposable  $\text{SiO}_2$  nanoparticles, we demonstrated sustained drug release in a controllable manner. The double loading of the drugs was achieved using two different mechanisms—the first one *via* a co-growth mechanism, and the second one by absorption. A two-phase sustained drug release was firstly revealed in an *in vitro* system, and then further demonstrated in mice. After a single intravenous injection, the drug was controllably released from the nanoparticles into blood circulation with a  $T_{\max}$  of about 8 h, afterwards a long lasting release pattern was achieved to maintain drug systemic exposure with a plasma elimination half-life of approximately 28 h. We disclosed that the absorbed drug molecules contributed to the initial fast release for quickly reaching the therapeutic level with relatively higher plasma concentrations, while the “grown-in” drugs were responsible for maintaining the therapeutic level *via* the later controlled slow and sustained release. The present nanoparticle carrier drug configuration and the loading/maintenance release mechanisms provide a promising platform that ensures a prolonged therapeutic effect by controlling drug concentrations within the therapeutic window—a sustained drug delivery system with a great impact on improving the management of chronic diseases.

Received 8th May 2015,  
Accepted 27th August 2015  
DOI: 10.1039/c5nr03029c  
[www.rsc.org/nanoscale](http://www.rsc.org/nanoscale)

## Introduction

Nanoparticles (NPs) serve as promising carriers for various cargos such as drugs due to their many advanced properties including enhanced cellular uptake,<sup>1,2</sup> and easiness to be equipped with multiple functionalities.<sup>3</sup> One of the most important issues in nanoparticle–carrier drugs is the release of the drug molecules from the carrier. In particular, sustained release is a critical feature that is desired in modern drug design. It aims to prolong the therapeutic effect and avoid the systemic toxic effect caused by burst release. Unlike conventional therapies, which show a saw-tooth type of drug concentration evolution in plasma, a sustained drug delivery system is designed to maintain therapeutic levels during the treatment period.

Over the years, a number of NP systems, including liposomes,<sup>4</sup> polymer NPs,<sup>5,6</sup> and inorganic NPs<sup>7</sup> have been investi-

gated in order to understand the drug release pattern from the NP carriers, aiming at sustained delivery of the drugs they carried. It has been found that the drug release is closely related to both the properties of the drug carrier and how the drugs were loaded onto the NP carriers. In the case of a liposome, drug molecules could be either housed in its hollow center or inserted into the lipid membrane. The gradual release of the drug molecules from a liposome is mainly driven by diffusion. Typically, the drug molecules need to diffuse out through the membrane. The drug release rate is determined by the physicochemical properties of the liposome, and the strategies utilized for drug loading, as well as the characters of the loaded drugs. A challenge with the liposome based drug originates from its easily deformed/destroyed lipid bilayer in bio-environment, causing rapid premature drug release from the carrier in the biological system.<sup>8,9</sup> Another major category of drug carriers is polymeric NPs, the most representative of which is known as biodegradable poly (lactic-co-glycolic) acid (PLGA) NPs. Drug molecules are uniformly embedded in the polymeric matrix or reside inside the polymeric shells. The rate of drug release can be manipulated by tuning the polymer degradation rate.<sup>10</sup> Such degradation results from hydrolysis of polymer,<sup>11</sup> and the rate of this process is highly dependent on the polymeric matrix's property (*e.g.* accessibility of water to the PLGA matrix). Moreover, the degradation process involves NP erosion that reduces the sizes of the NPs. This may cause NPs' quick clearance from the bio-

<sup>a</sup>Department of Physics, The Chinese University of Hong Kong, Shatin, New Territory, Hong Kong, China. E-mail: liquan@phy.cuhk.edu.hk

<sup>b</sup>School of Biomedical Sciences, Faculty of medicine, The Chinese University of Hong Kong, Shatin, New Territory, Hong Kong, China

<sup>c</sup>Department of Pharmaceutical Analysis, School of Pharmacy, Fourth Military Medical University, Xi'an, China

† Electronic supplementary information (ESI) available. See DOI: 10.1039/c5nr03029c

‡These authors contributed equally to this work.

logical system, leading to incomplete release of drugs *in vivo*. Inorganic NPs, such as mesoporous silica NPs, carbon NPs and iron oxide NPs have also been employed as drug carriers to realize sustained drug release.<sup>12–16</sup> The drug molecules reside in the pores or hollow center of the NPs. The sustained release of drugs can be controlled by manipulating the pore morphologies and/or applying surface capping. However, the non-decomposable inorganic NPs may have a risk of increasing potential toxicity at the system level, as the NP carriers may accumulate in organs (*i.e.* the mononuclear phagocytic system-related organs such as the liver and the spleen) and their excretion from bio-systems need a long time. In view of this fact, some degradable NP systems have been developed, such as mesoporous organosilica, porous silicon, calcium phosphate, zinc sulfide, zinc oxide, magnesium phosphate and manganese phosphate NPs.<sup>17–21</sup> However, these systems either involve other organic materials during relatively complicated synthesis, or face the problem of quick degradation and premature drug release, which requires a further development of surface coating/capping.

In the present work, we designed a double loading scheme using a specific type of NP, and achieved a two-phase sustained release with a fast initial release to reach the therapeutic level followed by a long lasting release pattern. We have employed amorphous silica NP as the drug carrier, as it is generally accepted as non-toxic,<sup>22,23</sup> and provides a versatile platform for drug delivery.<sup>24</sup> We double loaded the SiO<sub>2</sub> NPs with the same drug molecules but *via* different loading mechanisms, *i.e.*, “grown-in” and “absorbed”. The first load of the NPs was realized by introducing the drug molecules during the SiO<sub>2</sub> NP growth, and the second was carried out by soaking the first-loaded NPs into the solution containing the same drug molecules. As a result, the “absorbed” drug molecules ensured high therapeutic level at the beginning of the treatment, while the “grown-in” drug molecules were responsible for maintaining the therapeutic level for longer durations. Combining the two generates an ideal two-phase sustained drug release profile, *i.e.* an initial fast release reaching the therapeutic level, and the drug plasma concentration maintenance afterwards, showing great advantage to the pure drug counterpart. By varying the synthetic parameters during the NP growth, we were able to manipulate the release profiles of the drug in a large range. In addition, the “grown-in” drug molecules are also responsible for the self-decomposable feature of such NP-carrier drugs—after the drug molecules are completely released from the NPs, they can be decomposed into small fragments <5 nm, and were easily excreted from the renal system,<sup>25</sup> significantly reducing the system toxicity.

## Experimental

### Fabrication of the nanoparticles and different drug loading methods

SiO<sub>2</sub>-drug NPs (A Model: NPs with drug grown in the SiO<sub>2</sub> matrix) were first synthesized using a modified Stöber

method that has been reported elsewhere.<sup>25</sup> Bleomycin-A5 (BLM) or methylene blue (MB) were used as the model drug molecules. In a typical procedure of Model A, a certain amount of drug was added to a mixture of 75 mL ethanol and 3.4 mL 25% ammonia-water solution, and after that a certain amount of tetraethyl orthosilicate (TEOS) was added. The SiO<sub>2</sub>-drug NPs were obtained after 24 hours’ stirring, and washed several times before being dried. The actual drug amount grown into the NPs was calculated from the absorbance spectra changes before and after the reaction process, that is, grown-in drug amount in the NPs = Total reactant drug amount – drug amount in supernatant after NPs’ separation and washing. Calibration of the drug amount dependence on its absorbance spectra can be found in the ESI (Fig. S1†).

In A Model, two series of samples were prepared. In the first series, the TEOS amount (denoted as  $T$ ) was kept the same ( $T_{--} = 0.15$  mL), while the “grown-in” drug amounts (denoted as CIn) were changed from CIn<sub>–</sub> = ~1 μmol for sample A<sub>CIn<sub>–</sub></sub>,  $T_{--}$ , to CIn = ~2.2 μmol for sample A<sub>CIn</sub>,  $T_{--}$ , and to CIn<sub>+</sub> = ~3.7 μmol for sample A<sub>CIn<sub>+</sub></sub>,  $T_{--}$ . In the second series, the grown-in drug amount was kept at CIn = ~2.2 μmol, while the TEOS amounts were changed from  $T_{--} = 0.15$  mL for sample A<sub>CIn</sub>,  $T_{--}$ , to  $T = 0.2$  mL for sample A<sub>CIn</sub>,  $T$ , and to  $T = 0.23$  mL for sample A<sub>CIn</sub>,  $T$ .

Dual loaded NPs with grown-in MB and absorbed BLM (B model) were obtained by immersing SiO<sub>2</sub>-MB NPs in a BLM solution and stirred for 24 hours in order to absorb BLM. The actual BLM amount absorbed into the NPs was calculated by the equation: Absorbed BLM amount in the NPs = Total BLM amount in solution – BLM amount in supernatant after NPs’ separation and washing. Two series of samples were prepared. In the first series, both TEOS and grown-in MB amounts of SiO<sub>2</sub>-MB NPs were kept the same ( $T_{--} = 0.15$  mL, CIn = ~2.2 μmol), while the absorbed BLM amount (denoted as CAB) was changed from CAB<sub>–</sub> = ~0.5 μmol for sample B<sub>CIn</sub>,  $T_{--}$ , CAB<sub>–</sub>, to CAB = ~0.8 μmol for sample B<sub>CIn</sub>,  $T_{--}$ , CAB, and to CAB<sub>+</sub> = ~1.0 μmol for sample B<sub>CIn</sub>,  $T_{--}$ , CAB<sub>+</sub>. In the second series, both the grown-in MB and the absorbed BLM amounts were kept the same (CIn = ~2.2 μmol and CAB = ~0.8 μmol), while the TEOS amount was changed from  $T_{--} = 0.15$  mL for sample B<sub>CIn</sub>,  $T_{--}$ , CAB<sub>–</sub>, to  $T = 0.2$  mL for sample B<sub>CIn</sub>,  $T$ , CAB<sub>–</sub>, and to  $T = 0.23$  mL for sample B<sub>CIn</sub>,  $T$ , CAB<sub>+</sub>.

Double loaded NPs with both grown-in BLM and absorbed BLM (D model) were synthesized by immersing SiO<sub>2</sub>-BLM NPs in BLM solution and stirred for 24 hours in order to absorb BLM. Both the grown-in BLM and the absorbed BLM amounts were kept the same (CIn = ~2.2 μmol and CAB = ~0.8 μmol), while the TEOS amount was changed from  $T_{--} = 0.15$  mL for sample D<sub>CIn</sub>,  $T_{--}$ , CAB<sub>–</sub>, to  $T = 0.2$  mL for sample D<sub>CIn</sub>,  $T$ , CAB<sub>–</sub>, and to  $T = 0.23$  mL for sample D<sub>CIn</sub>,  $T$ , CAB<sub>+</sub>.

All samples were washed several times before being dried. The dried BLM-SiO<sub>2</sub>-BLM NPs, BLM-SiO<sub>2</sub>-MB NPs, SiO<sub>2</sub>-BLM NPs and SiO<sub>2</sub>-MB NPs were then stored for further drug release studies.

## In vitro studies of drug release and carrier decomposition process

The drug release was examined by dispersing 15 mg NPs in 5 mL deionized water and incubating at 37 °C for a certain amount of time. The supernatant was separated from the NPs by centrifugation (12 000 rpm) every day to measure the day-by-day drug release amount using a Hitachi U-3501 UV-vis-NIR spectrophotometer. Then the separated NPs were re-dispersed into 5 mL fresh deionized water to continue the drug release process. Such measurements were repeated every day until the drug was completely released from the NPs. All measurements were conducted in triplicate and the mean values with standard deviations were reported. The cumulative release amount of drug was calculated by summing up every day's drug release amount. The degradation of SiO<sub>2</sub> carriers was monitored by morphology investigation using transmission electron microscopy (TEM, Philips CM120).

## In vivo studies of drug release from NPs

Double loaded NPs (*e.g.* BLM–SiO<sub>2</sub>–BLM NPs,  $T = 0.23$  mL, CIn =  $\sim 2.2$  μmol, and CAB =  $\sim 0.8$  μmol) were used to evaluate the drug release profile *in vivo*. Male Sprague-Dawley (SD) rats ( $160 \pm 10$  g) were supplied by the Laboratory Animal Service Center, The Chinese University of Hong Kong. Animals were housed under standard conditions of temperature, humidity and light. Food and water were provided *ad libitum*. Rats in two groups ( $n = 3$  in each group) were injected intravenously with 0.2 mL of pure BLM or BLM–SiO<sub>2</sub>–BLM NPs, respectively, at the same BLM dose ( $2.67$  mg kg<sup>-1</sup>) through the tail vein. Blood ( $\sim 1$  mL) was drawn from rats and put into heparinized Eppendorf tubes at different time intervals (0.5, 4, 8, 24, 48, 72, and 80 hours after injection). The blood sample was centrifuged at 4 °C, 8000 rpm immediately and 0.5 mL of plasma was harvested. Each plasma sample (0.5 mL) was mixed with 0.5 mL of 20% perchloric acid, vortexed, and centrifuged at 15 000g for 5 min. The supernatant was collected to measure the BLM concentrations using the above mentioned UV-vis-NIR spectrophotometer.

The *in vivo* drug release profiles of A model (*e.g.* SiO<sub>2</sub>–BLM NPs,  $T = 0.23$  mL, CIn =  $\sim 2.2$  μmol) and B model (BLM–SiO<sub>2</sub>–MB NPs,  $T = 0.23$  mL, CIn =  $\sim 2.2$  μmol, and CAB =  $\sim 0.8$  μmol) were also evaluated using the same experimental protocol. Rats were injected with NPs or pure BLM, at the same BLM dose (A Model: 1.95 mg kg<sup>-1</sup>, B Model: 0.72 mg kg<sup>-1</sup>).

All experiments and animal care were conducted in accordance with the International Guiding Principles for Biomedical Research Involving Animals and the Hong Kong Code of Practice for Care and Use of Animals for Experimental Purposes, and were approved by Animal Experimental Ethics Committee of the Chinese University of Hong Kong.

## Results and discussion

Double loading of the NPs was achieved *via* two different mechanisms. The first load was realized by introducing the

drug molecules during the growth of SiO<sub>2</sub> NPs.<sup>25</sup> In such NPs, the drug was most concentrated in the center of the nanoparticle with a radial concentration gradient, the feature which makes the NPs self-decomposable.<sup>25</sup> We name this part of the drug as “grown-in”. The second load of the NPs was then achieved by absorbing the same drug onto self-decomposable NPs. We name this part of the drug as “absorbed”. A schematic to illustrate the configuration of the double-loaded NPs was shown in Fig. 1a.

Taking bleomycin-A5 (BLM) as a model drug, double loaded BLM–SiO<sub>2</sub>–BLM NPs were synthesized (D model). Fig. 1b shows morphology of such NPs, which are spherical in shape and have an average diameter of  $\sim 80$  nm. Successful loading of the BLM into the SiO<sub>2</sub> NPs were suggested by the optical absorption spectra taken at different stages of the loading process. In Fig. 1c, the first load (grown-in BLM) gave an obvious optical absorption peak at 290 nm, matching that of pure BLM and being absent in the case of pure SiO<sub>2</sub>. The second load (absorbed BLM) led to a jump in the BLM optical absorption intensity, suggesting additional loading of BLM to the NPs.

The release profile of BLM from the BLM–SiO<sub>2</sub>–BLM NPs (named as D-profile) (Sample D<sub>CIn, T, CAB</sub>: NPs synthesized with tetraethyl orthosilicate (TEOS) amount:  $T = 0.23$  mL; the grown-in drug amount: CIn =  $\sim 2.2$  μmol, and the absorbed drug amount: CAB =  $\sim 0.8$  μmol) was examined by immersing them in deionized water at 37 °C. Optical absorption spectra were recorded from the supernatant to measure the amount of BLM released every day. Fig. 1d and e plotted the BLM release profiles in both day-by-day and cumulative styles (*e.g.* “Profile D<sub>CIn, T, CAB</sub>” represents the D-profile taken from sample D<sub>CIn, T, CAB</sub>). In Fig. 1d, after an initial quick rise in the amount of drug released at Day 1, an obvious plateau appeared in the profile and lasted from Day 2 to Day 7, disclosing the stable amount of drug release daily and showing the maintenance of stable drug concentration level for 6 days. Such a characteristic of long sustained release can also be observed in the cumulative release profile, as shown in Fig. 1e.

Together with the drug release, continuous morphological evolution of the BLM–SiO<sub>2</sub>–BLM NPs was also observed using transmission electron microscopy (TEM) (Fig. 1f–i). Most of the NPs remained intact on day 1 (Fig. 1f), while obvious hollow features appeared in the center of many of the NPs after 4 days of immersion in deionized water (Fig. 1g). At the same time, the structure appeared porous. Such a uniform center-hollow feature continued to enlarge in the following days, leaving a spherical shell with thinner and thinner shell thickness. At day 10, some of the nanoshells appeared as partially damaged (Fig. 1h), and even longer duration (after 16 days) led to complete collapse of the nanoshell structure to scattered fragments (Fig. 1i). Such self-decomposable feature was not observed in pure SiO<sub>2</sub> NPs (Fig. S2†). The center-out release pattern of the “grown-in” BLM enabled the maintenance of the carrier size integrity until all drug molecules were released, avoiding incomplete drug release before carrier excretion.

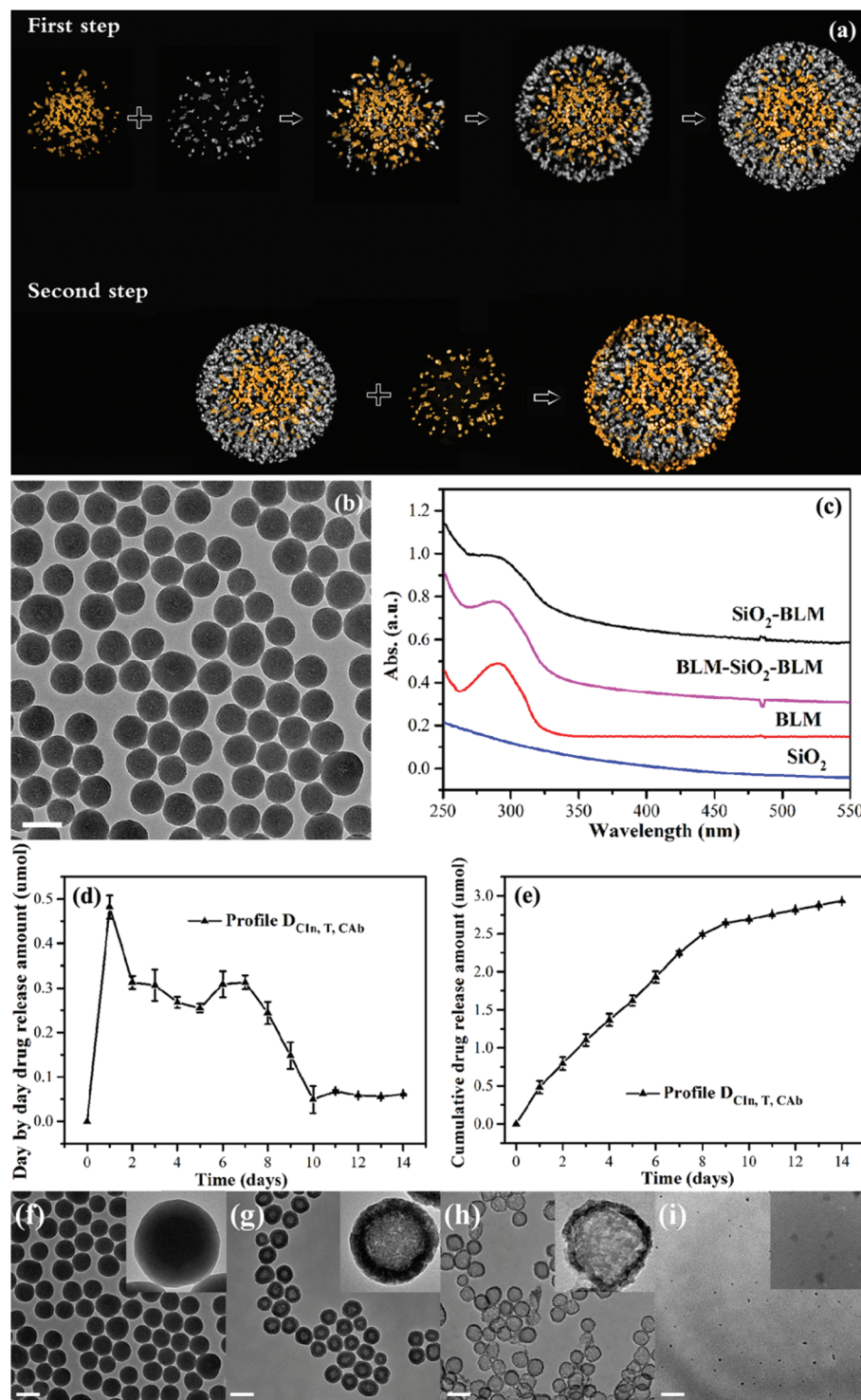


**Fig. 1** (a) A schematic to illustrate the loading process of the double-loaded NPs (D model); (b) low magnification TEM image of the as-synthesized NP. The scale bar is 100 nm; (c) optical absorption spectra taken from pure  $\text{SiO}_2$ , pure BLM,  $\text{SiO}_2\text{-BLM}$  NPs, and  $\text{BLM-SiO}_2\text{-BLM}$  NPs; (d, e) day-by-day and cumulative profiles of BLM release from  $\text{BLM-SiO}_2\text{-BLM}$  NPs. TEM images of the  $\text{BLM-SiO}_2\text{-BLM}$  NPs after being immersed in deionized water at 37 °C for (f) 1, (g) 4, (h) 10, and (i) 16 days. The scale bar is 100 nm. The corresponding high resolution images are inserted respectively in the upper right corner. The experimental data shown in these figures were obtained from  $\text{BLM-SiO}_2\text{-BLM}$  NP (sample  $D_{\text{Cln}, \text{T}, \text{CAB}}$ ) synthesized with TEOS amount of 0.23 mL, first-loaded BLM amount  $\sim 2.2 \mu\text{mol}$ , and second-loaded BLM amount  $\sim 0.8 \mu\text{mol}$ .

Furthermore, the sustained drug release profile of BLM–SiO<sub>2</sub>–BLM NPs was investigated in the rats treated with a single intravenous injection of BLM–SiO<sub>2</sub>–BLM NPs or BLM at the same dose of BLM. As depicted in Fig. 2, the BLM–SiO<sub>2</sub>–BLM NPs demonstrated a controllable release of BLM to reach the maximum plasma concentration at about 8 h. Afterwards, a sustained release feature was observed for 3 days. The plasma elimination half-life was determined to be  $27.96 \pm 3.60$  h after reaching the peak concentration. These results further confirmed the prolonged release profile *in vivo*. In contrast, after intravenous injection of BLM, its plasma concentration rapidly dropped to an undetectable level within 24 h with a normal first-order kinetics elimination profile. In the present study, the *in vivo* sustained release effect of BLM–SiO<sub>2</sub>–BLM NPs is remarkable when compared to dosing BLM alone, indicating a promising application of BLM–SiO<sub>2</sub>–BLM NPs in drug delivery. It is noted that although the release patterns were the same, the rate of release of BLM from NPs was faster in the *in vivo* than in the *in vitro* system (Fig. 1d and 2). This phenomenon was expected, because unlike in the *in vitro* situation, the BLM released in the plasma would be immediately cleared through different elimination processes including rapid distribution into different compartments, its metabolism and excretion. Subsequently, the lower concentration of BLM in the vicinity of the NPs would facilitate the further release of the remaining BLM in BLM–SiO<sub>2</sub>–BLM NPs.

In order to understand such sustained release behavior, we carried out a number of control experiments in a systematic manner, and studied the release profiles of both the first-loaded, and the second-loaded BLM from the NPs.

The investigation of the first-loaded BLM was carried out in a NP model with BLM introduced only during the NP growth (A Model), *i.e.*, with exactly the same synthetic parameters as those of the BLM–SiO<sub>2</sub>–BLM NPs described above but only

first-loaded (grown-in) BLM being involved. Fig. 3a illustrates the configuration of such SiO<sub>2</sub>–BLM NP (Sample A<sub>CIn</sub>, *T* with CIn =  $\sim 2.2$   $\mu$ mol and *T* = 0.23 mL). Its morphology can be found in the TEM image shown in Fig. 3b (sample A<sub>CIn</sub>, *T*). Similar to the BLM–SiO<sub>2</sub>–BLM NPs, they were spherical in shape with an average diameter of  $\sim 80$  nm. Successful incorporation of BLM into the NPs was suggested by the optical absorption spectrum taken from the NP sample. The characteristic absorption of BLM at 290 nm was clearly observed in the SiO<sub>2</sub>–BLM NPs but not in the pure SiO<sub>2</sub> NPs (Fig. 3c).

The release profile of BLM from the SiO<sub>2</sub>–BLM NPs (A-profile) was also examined in the deionized water at 37 °C. Fig. 3d and e show the plotted BLM release profiles in both day-by-day and cumulative styles (*e.g.* “BLM Profile A<sub>CIn</sub>, *T*” represents A-profile of drug BLM taken from sample A<sub>CIn</sub>, *T*). A slow rise was observed in the first few days for the amount of BLM released into the supernatant. A peak release amount appeared at Day 6 (Fig. 3d), and  $\sim 100\%$  (2.15/2.2  $\mu$ mol) drug release was achieved at last (14 days) (Fig. 3e).

The peak position (*i.e.*, the peak release of the drug) in Fig. 3d was found to be affected by two experimental parameters. One is the concentration of BLM loaded. This was demonstrated by the results obtained from three SiO<sub>2</sub>–BLM samples with different BLM loading amount (*i.e.*, sample A<sub>CIn</sub>, *T*—, A<sub>CIn</sub>, *T*—, A<sub>CIn+</sub>, *T*—, with CIn<sup>—</sup> =  $\sim 1$   $\mu$ mol, CIn =  $\sim 2.2$   $\mu$ mol, and CIn<sup>+</sup> =  $\sim 3.7$   $\mu$ mol) but the same TEOS amount (*T*— = 0.15 mL). The corresponding peak position appeared at Day 3, Day 3, and Day 2 (Fig. S3a†). The drug amount was found to affect the release rate of BLM—a higher BLM amount led to a faster BLM release from the NPs. Such a trend can be clearly seen in the corresponding cumulative profiles in Fig. S3b.†

The other parameter affecting the position of the peak BLM release was the amount of TEOS introduced during the NP growth. This was demonstrated by the three BLM release profiles taken from SiO<sub>2</sub>–BLM samples (*i.e.*, sample A<sub>CIn</sub>, *T*, A<sub>CIn</sub>, *T*—, and A<sub>CIn</sub>, *T*—) with the decreasing TEOS amount (*T* = 0.23 mL, *T*— = 0.2 mL, and *T*— = 0.15 mL), BLM amount were all kept at CIn  $\sim 2.2$   $\mu$ mol. The corresponding peak position appeared at Day 3 for sample A<sub>CIn</sub>, *T*—, Day 4 for sample A<sub>CIn</sub>, *T*—, and Day 6 for sample A<sub>CIn</sub>, *T* (Fig. S4a†). The TEOS amount affected the density of the SiO<sub>2</sub> hosting network for BLM—a higher TEOS amount led to a denser SiO<sub>2</sub> network and thus slower BLM release from the NPs. Such a trend can be clearly seen in the corresponding cumulative profiles in Fig. S4b.†

Similar results were obtained when one replaced BLM with a different drug, *e.g.* methylene blue (MB) (Fig. S5a†). TEM image and optical absorption spectrum taken from SiO<sub>2</sub>–MB NPs are shown in Fig. S5b and S5c,† respectively. Successful incorporation of the MB into the NPs was suggested by the optical absorption spectrum recorded from the NPs. The characteristic absorption of MB at 660 nm (for monomer) and 600 nm (for dimer) were clearly observed in the SiO<sub>2</sub>–MB NPs but not in the pure SiO<sub>2</sub> NPs (Fig. S5c†). The day-by-day and cumulative MB release profiles were plotted (Fig. S5d and S5e†), and the adjustable peak position of MB release amount

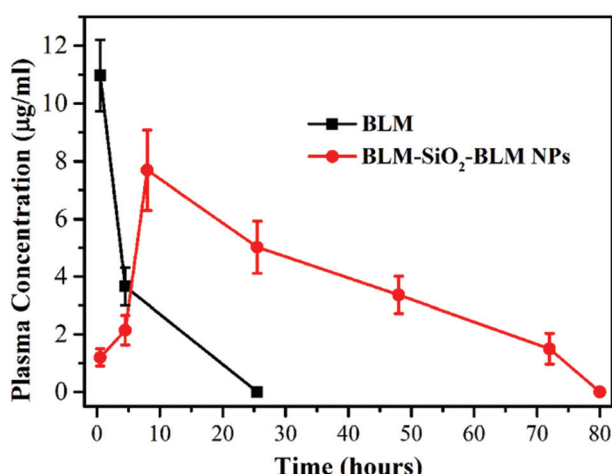
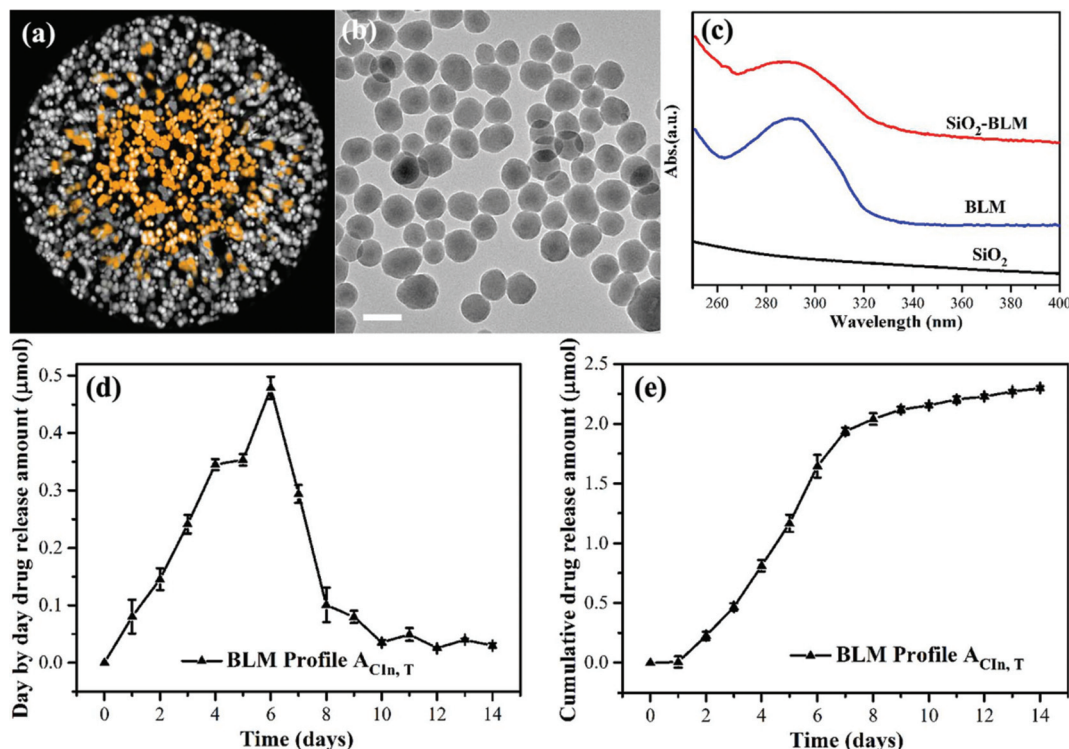


Fig. 2 The BLM concentration in plasma after the injection of pure drug and BLM–SiO<sub>2</sub>–BLM NPs. Each data point represents the mean  $\pm$  SD of three rats.



**Fig. 3** (a) Illustration of the SiO<sub>2</sub>–BLM self-decomposable NP (A Model); (b) low magnification TEM image of the as-synthesized SiO<sub>2</sub>–BLM NP (sample A<sub>CIn, T</sub>). The scale bar is 100 nm; (c) optical absorption spectra taken from pure SiO<sub>2</sub>, pure BLM, and SiO<sub>2</sub>–BLM NPs; (d, e) day-by-day and cumulative release profiles of BLM in deionized water from A Model NPs at 37 °C. The experimental data shown in this figure were obtained from the SiO<sub>2</sub>–BLM NP (sample A<sub>CIn, T</sub>) synthesized at TEOS amount of  $T = 0.23$  mL, first-loaded (grown-in) BLM amount  $\sim 2.2$  μmol.

was also shown (*e.g.* “MB Profile A<sub>CIn, T</sub>” represents A-profile of drug MB taken from sample A<sub>CIn, T</sub>). In these samples, the same amount of MB (molar) was incorporated into the SiO<sub>2</sub> at exactly the same synthetic conditions as those of SiO<sub>2</sub>–BLM NPs (sample A<sub>CIn, T</sub>–, A<sub>CIn, T</sub>–, and A<sub>CIn, T</sub>). The similar release pattern of the drug molecules observed from both SiO<sub>2</sub>–MB and SiO<sub>2</sub>–BLM NPs suggested that the drug release from the NPs which only involved first-loaded (grown-in) drug (A-profile) was dependent on the drug molar amount.

The *in vivo* studies were also conducted for the A model, and the BLM release profile is shown in Fig. S6a.† The SiO<sub>2</sub>–BLM NPs demonstrated a slow release of BLM to reach the maximum concentration at about 24 h and to be eliminated from the body with the half-life of about 16 h.

The investigation of the second-loaded (absorbed) BLM was carried out in a NP model by dual loading of MB (grown-in) and BLM (absorbed) in the same NP (B Model). Specifically, the SiO<sub>2</sub>–MB NPs (A Model, the same parameter as sample A<sub>CIn, T</sub>, CIn =  $\sim 2.2$  μmol and  $T = 0.23$  mL) was synthesized first and the BLM was then loaded *via* absorption (named as BLM–SiO<sub>2</sub>–MB NP, B Model, sample B<sub>CIn, T, CAB</sub>, with CAB representing the absorbed BLM amount, here CAB =  $\sim 0.8$  μmol). The release profile of the absorbed BLM was named as B-profile (*e.g.* “Profile B<sub>CIn, T, CAB</sub>” represents B-profile taken from sample B<sub>CIn, T, CAB</sub>). To differentiate the MB release profile from that in

A Model, here we name the MB release profile in this B Model as the DA-profile (*e.g.* “Profile DA<sub>CIn, T, CAB</sub>” represents DA-profile taken from sample B<sub>CIn, T, CAB</sub>). Illustration of the BLM–SiO<sub>2</sub>–MB NP configuration is shown in Fig. 4a. MB was concentrated in the center and had a concentration gradient along the NP’s radial direction. BLM was mostly absorbed in the vicinity of NP’s surface region. The morphology of the as-synthesized BLM–SiO<sub>2</sub>–MB NPs is shown in Fig. 4b, being very similar to the NPs described earlier. Successful incorporation of both BLM and MB in the NPs was suggested by the optical absorption spectra recorded from the BLM–SiO<sub>2</sub>–MB NP sample (Fig. 4c).

Being different from A-profile (release of the grown-in BLM) in A Model, the B-profile (release of the absorbed BLM) showed a high initial burst of release followed by a quick drop, *i.e.*, a sharp peak was observed at Day 1 in the day-by-day plot and the amount of drug released quickly went down afterwards (Fig. 4d). The initial release burst was caused by the diffusion of the BLM loaded in the surface/subsurface layer of NPs.<sup>26,27</sup>

The peak position in Fig. 4d was not sensitive to the amount of BLM incorporated (Fig. S7a†), as suggested by the day-by-day release profiles taken from three BLM–SiO<sub>2</sub>–MB NP samples with all other parameters being the same but with different amounts of BLM (samples B<sub>CIn, T</sub>–, CAB–, B<sub>CIn, T</sub>–, CAB and B<sub>CIn, T</sub>–, CAB+ with CAB– =  $\sim 0.5$  μmol, CAB =

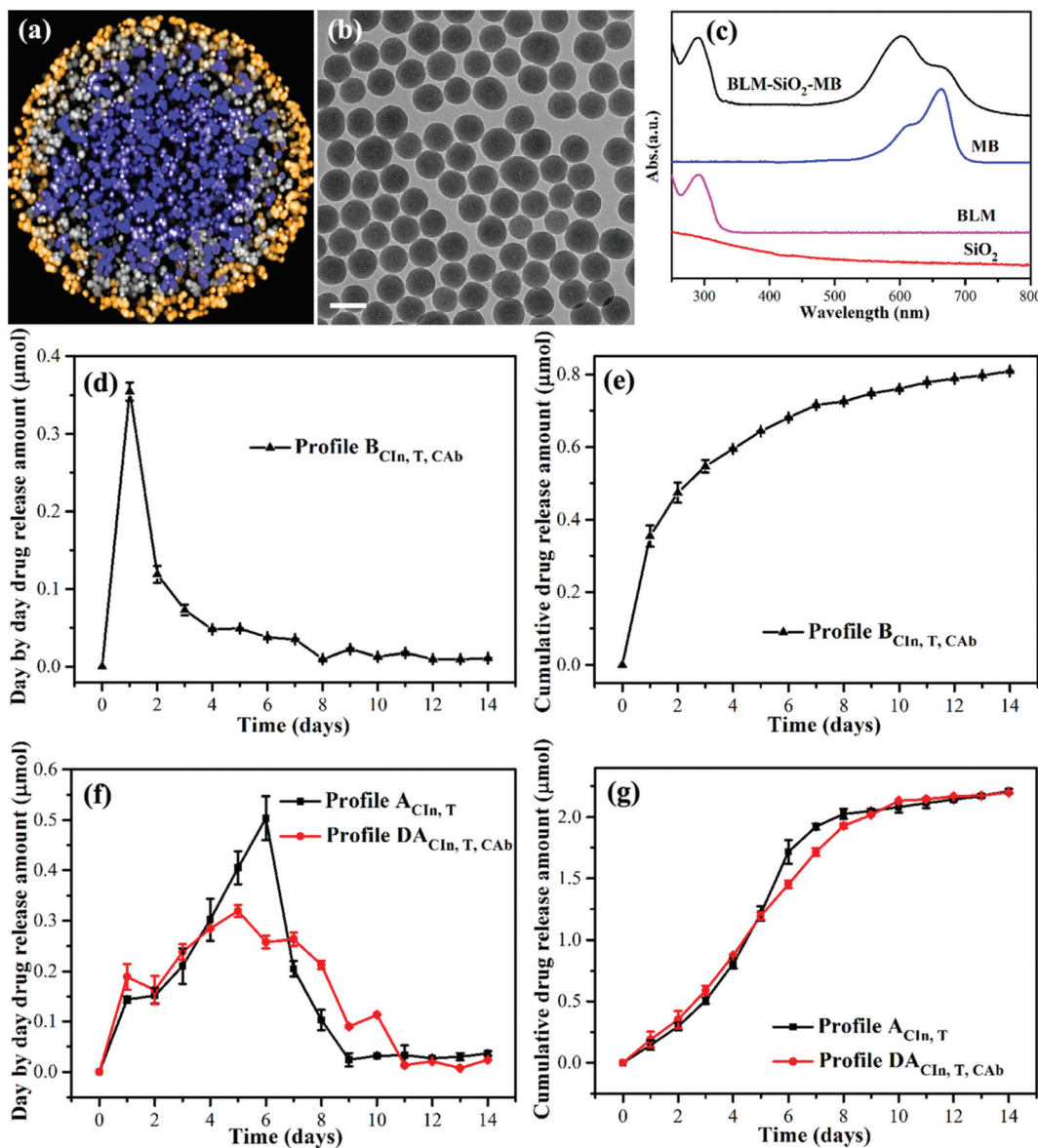


**Fig. 4** (a) Illustration of the BLM–SiO<sub>2</sub>–MB NP configuration (B Model); (b) low magnification TEM image of the as-synthesized BLM–SiO<sub>2</sub>–MB NPs. The scale bar is 100 nm; (c) optical absorption spectra taken from pure SiO<sub>2</sub>, pure BLM, and BLM–SiO<sub>2</sub>–MB NPs; (d) day-by-day and (e) cumulative release profiles of BLM from NPs; (f) day-by-day and (g) cumulative release profiles of MB from SiO<sub>2</sub>–MB and BLM–SiO<sub>2</sub>–MB NPs (A profile and DA-profile). The sample B<sub>CIn, T, CAB</sub> synthetic parameters were: grown-in MB amount CIn = ~2.2 μmol, TEOS amount T = 0.23 mL, and absorbed BLM amount CAB = ~0.8 μmol.

~0.8 μmol, and CAB+ = ~1.0 μmol, respectively). The corresponding cumulative release profiles of BLM are shown in Fig. S7b.† One can easily identify the initial burst release and then the quickly achieved ~100% (0.47/0.5 μmol, 0.75/0.8 μmol and 0.94/1.0 μmol) release afterwards in all of the samples.

The peak position in Fig. 4d was also not sensitive to the TEOS amount during NP growth (Fig. S8a†), as suggested by day-by-day release profiles taken from the three BLM–SiO<sub>2</sub>–MB NP samples (sample B<sub>CIn, T–, CAB</sub>, B<sub>CIn, T–, CAB</sub>, and B<sub>CIn, T, CAB</sub>) with all other parameters being the same but with different TEOS amounts (T– = 0.15 mL, T– = 0.2 mL, and T =

0.23 mL). The corresponding cumulative release profiles of BLM are shown in Fig. S8b.† One can easily identify the initial burst in release and then the quickly achieved ~100% (0.75/0.8 μmol) release afterwards in all three samples.

On the other hand, the load of BLM (absorbed) into the SiO<sub>2</sub>–MB NPs was found to affect the release pattern of MB. Fig. 4f and g compared the DA-profile (release profile of MB from the BLM–SiO<sub>2</sub>–MB NPs, sample B<sub>CIn, T, CAB</sub>) to the A-profile (release profile of MB from the SiO<sub>2</sub>–MB NPs, sample A<sub>CIn, T</sub>), with the MB amount and TEOS amount being the same in the two samples. In a sense, the release of MB was

"delayed" by the presence of the absorbed BLM. This was not surprising as the absorbed BLM molecules in the outer layer of NPs block the way of the MB release. Nevertheless, the amount of absorbed BLM (CAb<sup>-</sup>, CAb, and CAb<sup>+</sup> in Fig. S7†) did not further affect the release profile of the delayed MB profile taken from BLM–SiO<sub>2</sub>–MB NPs (Fig. S9†). That is likely due to the fact that the absorbed BLM have a high initial release at Day 1. After a substantial amount of the surface absorbed BLM was cleared, the blocking effect from the rest of the absorbed BLM became trivial.

The *in vivo* BLM release profile is shown in Fig. S6b.† The BLM–SiO<sub>2</sub>–MB NPs (Fig. S6b†) showed a relatively quick initial drug release with the  $T_{\max}$  at about 8 h, and a rapid elimination with the half-life of about 11 h. On the other hand, we also examined the MB release profile in the B model, illustrating a slow release of MB with the  $T_{\max}$  at about 24 h and a zero-order kinetic elimination in the next two days (Fig. S10†). This result excluded the possibility of quick elimination of the NPs themselves (when the grown-in drugs were not released from the circulation (Fig. S10†).

By summing the DA-profile (MB release from BLM–SiO<sub>2</sub>–MB NPs, sample B<sub>CIn</sub>, T, CAb in Fig. 4f) and the B-profile (BLM release from BLM–SiO<sub>2</sub>–MB NPs, in Fig. 4d), one can largely reproduce the D profile (BLM release from the BLM–SiO<sub>2</sub>–BLM NPs, sample D<sub>CIn</sub>, T, CAb in Fig. 1d). This is shown in Fig. 5a and b. Therefore the release of BLM from BLM–SiO<sub>2</sub>–BLM NPs can be roughly understood as the summation from two release processes, *i.e.*, leaving of the absorbed BLM, and escape of the grown-in BLM, while the absorbed BLM indeed affect the release pattern of the grown-in one.

The role of the grown-in BLM was revealed by the characterization of the A model. One can observe a rather slow release profile of A model (Fig. 3e)—it took a while for the drug release to peak at day 6 and then gradually decreased. Together with the drug release, carriers underwent decomposition (Fig. S11†). The carrier decomposition was actually triggered by the drug release process. This was supported by experimental evidence from a control experiment, *i.e.*, by dispersing the SiO<sub>2</sub>–BLM NPs into acetone, in which BLM was not soluble, neither the BLM release nor the SiO<sub>2</sub> NP

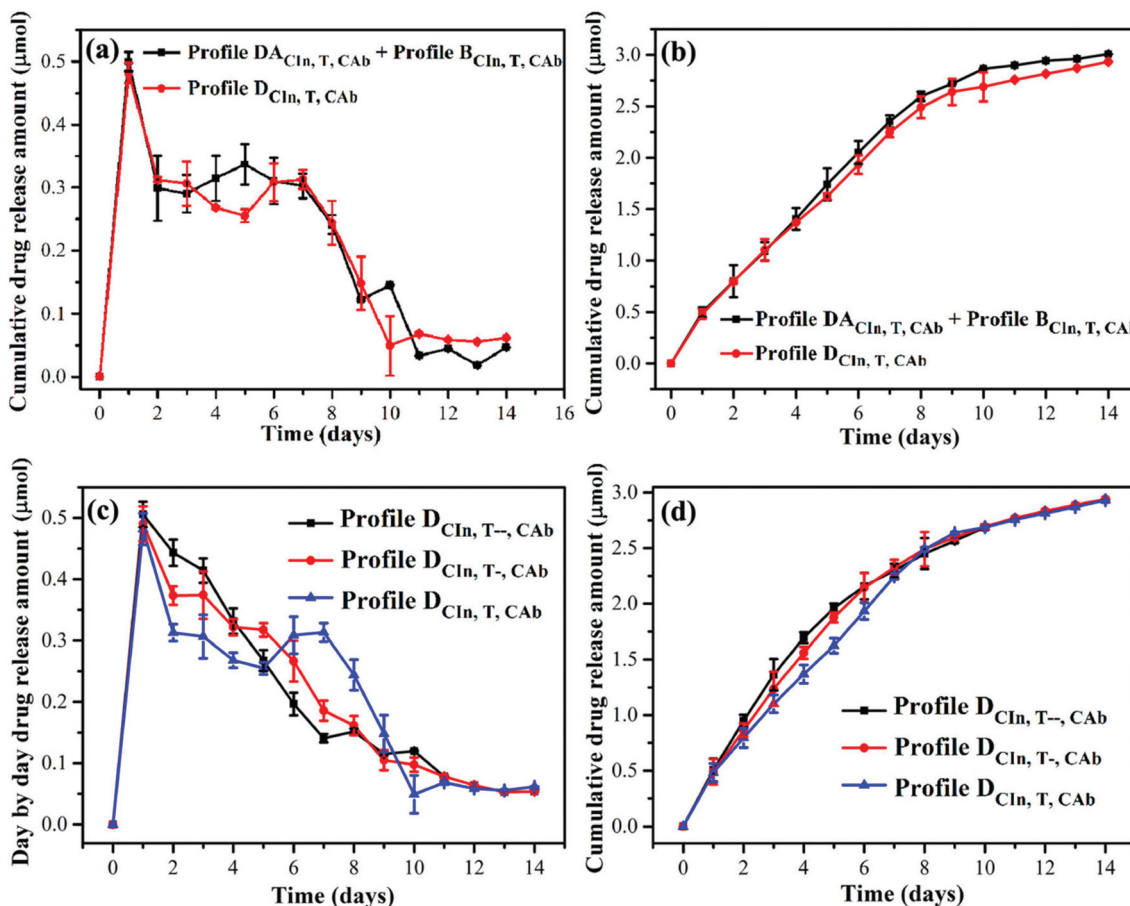


**Fig. 5** (a) Day-by-day and (b) cumulative release profile of D<sub>Cln, T, CAB</sub> profile compared to the summation of Profile DA<sub>Cln, T, CAB</sub> + Profile B<sub>Cln, T, CAB</sub> (Cln = ~2.2 μmol, CAb = ~0.8 μmol, and T = 0.23 mL). (c) Day-by-day and (d) cumulative release profiles of BLM taken from three BLM–SiO<sub>2</sub>–BLM NPs samples at the same BLM load amount (Cln = ~2.2 μmol, CAb = ~0.8 μmol) but different TEOS amount (T<sup>-</sup> = 0.15 mL, T<sup>-</sup> = 0.2 mL, and T = 0.23 mL).

decomposition occurred (Fig. S12†). In fact, the  $\text{SiO}_2$ -BLM NP was very stable after being dried—neither BLM escape nor  $\text{SiO}_2$  decomposition occurred after months when they were stored in the powder form.

The adsorbed drug's retardation effect on the release of the grown-in drugs could be observed in Fig. 4f. The DA-profile (release profile of MB from the BLM- $\text{SiO}_2$ -MB NPs, sample  $B_{\text{CIn}}$ ,  $T_{\text{cAB}}$ ) was compared to the A-profile (release profile of MB from the  $\text{SiO}_2$ -MB NPs, sample  $A_{\text{CIn}}$ ,  $T$ ), with the MB amount ( $\text{CIn}$ ) and TEOS amount ( $T$ ) being the same in the two samples. It was observed that the release of inner MB was “retarded” by the presence of the absorbed BLM—the peak release of  $A_{\text{CIn}}$ ,  $T$  at day 6 was suppressed, followed by increased MB release after day 6 in  $D_{\text{CIn}}$ ,  $T_{\text{cAB}}$ .

Manipulating the release profile of the drug can be realized by varying the TEOS amount during the synthesis of NPs. For example, Fig. 5c and d showed the change in the BLM release profile taken from BLM- $\text{SiO}_2$ -BLM NPs (D-profiles) when the TEOS amount is changed from  $T_{\text{--}} = 0.15$  mL to  $T_{\text{--}} = 0.2$  mL, and to  $T = 0.23$  mL. The sustained release profile with a longer plateau was realized by increasing TEOS amount. A closer look at the D-profile suggested the existence of three distinctive zones, namely the burst release, the stable release, and lastly complete release of drug. The first relatively high release rate was attributed to the diffusion of the absorbed BLM from the  $\text{SiO}_2$  surface/subsurface layers. The stable release resulted from the grown-in BLM escaping the NPs from the center to the outside through  $\text{SiO}_2$  network. Then the decrease in drug release was observed after the NPs degraded into small pieces which allowing the completed drug release. Such sustained drug release profile provided an ideal solution for building “efficacy” and “safety” into the therapeutic mechanism.

## Conclusion

In conclusion, the long-term sustained drug release can be realized through double loading of drugs in a special type of silica NP carrier. The first loaded “grown-in” drug molecules enabled gradual release and triggered carrier decomposition, and the second loaded “absorbed” drug molecules gave a sufficient drug level at the beginning of release. The “absorbed” drug molecules also have a delaying effect on the release of inner “grown-in” drug molecules. On the other hand, the release rate of the “grown-in” drug was sensitive to the NP growth parameters, *i.e.*, the TEOS amount that determined the compactness of the silica matrix as well as the “grow-in” drug concentration. In our work, by controlling the initial release amount of the “absorbed” drug and manipulating the release rate of the “grown-in” drug by varying synthetic parameters during NP growth, we were able to manipulate the drug release profiles and achieved both the initial fast release and maintenance of the drug levels for a long duration. This is highly desired and has a great impact on improving the management of chronic diseases, which require long-term medication.

## Acknowledgements

We acknowledge the valuable suggestions from Zhiqin Chu and Chunyuan Zhang, and Xu Wu for helping us with the blood sampling. This work was supported by the HK Scholars Program, and the Direct Grant (project no. 4053074), and CUHK Mainline Research Scheme under project No. 4053127.

## References

- V. P. Torchilin, *Nat. Rev. Drug Discovery*, 2005, **4**, 145–160.
- Z. Chu, Y. Huang, Q. Tao and Q. Li, *Nanoscale*, 2011, **3**, 3291–3299.
- D. Peer, J. M. Karp, S. Hong, O. C. Farokhzad, R. Margalit and R. Langer, *Nat. Nanotechnol.*, 2007, **2**, 751–760.
- T. M. Allen and P. R. Cullis, *Adv. Drug Delivery Rev.*, 2013, **65**, 36–48.
- A. Kumari, S. K. Yadav and S. C. Yadav, *Colloids Surf., B*, 2010, **75**, 1–18.
- T. Thambi, V. G. Deepagan, H. Y. Yoon, H. S. Han, S.-H. Kim, S. Son, D.-G. Jo, C.-H. Ahn, Y. D. Suh, K. Kim, I. Chan Kwon, D. S. Lee and J. H. Park, *Biomaterials*, 2014, **35**, 1735–1743.
- N. Erathodiyil and J. Y. Ying, *Acc. Chem. Res.*, 2011, **44**, 925–935.
- M. S. Mufamadi, V. Pillay, Y. E. Choonara, L. C. Du Toit, G. Modi, D. Naidoo and V. M. K. Ndesendo, *J. Drug Delivery*, 2011, 2011.
- P. Zou, S. Stern and D. Sun, *Pharm. Res.*, 2014, **31**, 684–693.
- E. Balmayor, H. Azevedo and R. Reis, *Pharm. Res.*, 2011, **28**, 1241–1258.
- R. Dinarvand, N. Sepehri, S. Manoochehri, H. Rouhani and F. Atyabi, *Int. J. Nanomed.*, 2011, **6**, 877–895.
- B. G. Trewyn, C. M. Whitman and V. S. Y. Lin, *Nano Lett.*, 2004, **4**, 2139–2143.
- Z. Li, J. C. Barnes, A. Bosoy, J. F. Stoddart and J. I. Zink, *Chem. Soc. Rev.*, 2012, **41**, 2590–2605.
- J. Gu, S. Su, Y. Li, Q. He and J. Shi, *Chem. Commun.*, 2011, **47**, 2101–2103.
- K. Cheng, S. Peng, C. Xu and S. Sun, *J. Am. Chem. Soc.*, 2009, **131**, 10637–10644.
- X. Liu, Q. Hu, Z. Fang, Q. Wu and Q. Xie, *Langmuir*, 2009, **25**, 7244–7248.
- J. Croissant, X. Cattoën, M. W. C. Man, A. Gallud, L. Raehm, P. Trems, M. Maynadier and J.-O. Durand, *Adv. Mater.*, 2014, **26**, 6174–6180.
- J.-H. Park, L. Gu, G. von Maltzahn, E. Ruoslahti, S. N. Bhatia and M. J. Sailor, *Nat. Mater.*, 2009, **8**, 331–336.
- A. Schroeder, D. A. Heller, M. M. Winslow, J. E. Dahlman, G. W. Pratt, R. Langer, T. Jacks and D. G. Anderson, *Nat. Rev. Cancer*, 2012, **12**, 39–50.
- G. Bhakta, S. Mitra and A. Maitra, *Biomaterials*, 2005, **26**, 2157–2163.
- S. R. Bhattarai and N. Bhattarai, *J. Nanomed. Nanotechol.*, 2013, **4**, 170.

- 22 Z. Chu, Y. Huang, L. Li, Q. Tao and Q. Li, *Biomaterials*, 2012, **33**, 7540–7546.
- 23 B. Fadeel and A. E. Garcia-Bennett, *Adv. Drug Delivery Rev.*, 2010, **62**, 362–374.
- 24 L. Tang, T. M. Fan, L. B. Borst and J. Cheng, *ACS Nano*, 2012, **6**, 3954–3966.
- 25 S. Zhang, Z. Chu, C. Yin, C. Zhang, G. Lin and Q. Li, *J. Am. Chem. Soc.*, 2013, **135**, 5709–5716.
- 26 Y. Jiao, J. Guo, S. Shen, B. Chang, Y. Zhang, X. Jiang and W. Yang, *J. Mater. Chem.*, 2012, **22**, 17636–17643.
- 27 R. Luo, B. Neu and S. S. Venkatraman, *Small*, 2012, **8**, 2585–2594.